Transition metal elements as donor dopants in CdO

Kin Man Yu [1,2,*] Wei Zhu,[2,3] Ying Wang [1] Yajie Li,[2,4] Chaoping Liu [5] Guibin Chen,[6] and Wladek Walukiewicz[2,†]

[1]*Department of Physics, City University of Hong Kong, Kowloon, Hong Kong, 999077*

[2]*Materials Sciences Division, Lawrence Berkeley National Laboratory, Berkeley, California 94720, USA*

[3]*Department of Physics and The Center for Physical Experiments, University of Science and Technology of China, Hefei, Anhui 230026, People's Republic of China*

[4]*Guangdong Provincial Key Laboratory of Electronic Functional Materials and Devices, Huizhou University, Huizhou 516007, China*

[5]*Department of Physics, College of Science, Shantou University, Shantou, Guangdong 515063, China*

[6]*Physics Department and Jiangsu Key Laboratory for Chemistry of Low Dimensional Materials, Huaiyin Normal University, Jiangsu 223001, China*

(Received 9 April 2023; accepted 30 June 2023; published 13 July 2023)

CdO has been shown to achieve a high electron concentration N ($>10^{21}$ cm^{-3}) and at the same time a high mobility μ (>100 cm^2/V s) when doped with conventional shallow dopants (In or Ga), and consequently making it a transparent conducting oxide with very low resistivity $\rho < 10^{-4}$ Ω cm. In this work, the properties of CdO thin films doped with a series of transition metal elements (CdO:TM) with partially filled $3d$ and $4d$ shells, including Sc, Ti, V, Cr, Fe, Y, Mo, and W, were investigated. We find that doping with these TM elements can effectively increase the N in CdO to a maximum N ($N_{\max}$) of $\sim(7–12)\times10^{20}$ cm^{-3} with a dopant concentration $x_{\max}$ of 4–7 %. However, unlike CdO:In, the μ of CdO:TM films drops rapidly from >100 to <10 cm^2/Vs as the dopant concentration x increases, so that they can only achieve a minimum ρ of $\sim(1–2)\times10^{-4}$ Ω cm, ∼ a factor of 2–3 higher than that in CdO:In. As a result, free-carrier absorption and plasma reflection effects limit their optical transparency to <1200 nm. For most $3d$ TM dopants, a qualitatively higher d-donor level $E_{d,\text{donor}}$ gives rise to higher $E_{F,\max}$ or a higher $N_{\max}$. Although at low x, the optical band gap E_{opt} of CdO:TM follows the calculated values due to free-carrier effects, as x increases, E_{opt} values are significantly higher than the calculated values. This is believed to be an effect of the anticrossing interaction of the localized d-levels and the extended CdO conduction-band (CB) states, giving rise to a lower occupied E_- and an upper unoccupied E_+ subband. The restructured CBs have much flatter dispersion, which also results in a much higher effective mass m_e^*, hence it can also explain the much lower μ of CdO:TM films with high N.

DOI: 10.1103/PhysRevMaterials.7.074602

I. INTRODUCTION

Transparent conducting oxides (TCOs) are wide-gap oxide semiconductors with a high conductivity (10^3–10^4 S/cm) and optical transparency which have been widely used in recent years for various applications [1–6], such as photovoltaic solar cells, flat-panel displays, light-emitting diodes, and optoelectronic devices [7–13]. Up to now, Sn-doped In_2O_3 (ITO), F-doped SnO_2 (FTO), and Al-doped ZnO (AZO) have been the most extensively used TCOs [1,5,13–17]. Although these conventional TCOs have high conductivity and good transparency over the visible and ultraviolet parts of the solar spectrum, due to their high electron concentration and low mobility, which give rise to strong free-carrier absorption and plasma reflection at $\lambda > 1000$ nm, their transparency for the long-wavelength photons is limited. This drawback limits their application in devices that utilize near-infrared photons, such as Si PVs and high efficiency multijunction solar cells. To extend the applications of these TCOs, their mobility must be improved so that a high conductivity can be attained with only moderate electron density. Recent reports demonstrated that instead of Sn doping, In_2O_3 can achieve much higher mobility when doped with transition metal (TM) dopants (such as Mo, W, Ti, and Zr) [18–24] and H [25–27]. Similar mobility enhancement was also reported for SnO_2 doped with TM dopant Ta [28]. In particular, Swallow *et al.* reported Mo-doped In_2O_3 thin films with a resistivity of $<10^{-4}$ Ω cm and a mobility as high as 150 cm^2/Vs grown by chemical vapor deposition [20]. This enhanced mobility in In_2O_3 was explained by the Mo $4d$ donor states being resonant in the conduction band of In_2O_3, and hence it does not modify the conduction-band dispersion.

Recently, CdO has received considerable attention because of its high mobility and electron concentration [29,30]. It has been shown that appropriately doped CdO can have electron concentration exceeding 10^{21} cm^{-3} and still has a mobility higher than any of the previously studied TCOs [30–32]. Electrical and optical properties of the CdO doped with various common group III donor species, including In, Ga, and Al, have been extensively studied [31,33–35], and these

*Corresponding author: kmyu@lbl.gov, kinmanyu@cityu.edu.hk
†Deceased.

common donors were demonstrated to be effective to increase the electron concentration to $>10^{21}$ cm^{-3} and still maintaining a high mobility of >100 cm^2/Vs. Hence, highly conducting CdO thin films with a resistivity $<10^{-4}\,\Omega$ cm and a high transparency >85 % over a wide spectral window of $400 < \lambda < 2000$ nm have been achieved. However, only a few works on the doping of CdO with transition TM dopants have been reported [31,36–39].

It has been shown that a TM element with $4s^2\,3d^n$ electronic configuration (e.g., Sc, Ti, V, Fe, Cr) can act as a donor when substituting cation atoms in II-VI compounds by changing its d-level configuration from $3d^n$ to $3d^{n-1}$. Because of the highly localized nature of d states, the energies of the donor levels remain constant relative to the vacuum level (E_{vac}) [40]. The energies of the donor levels vary from ∼−4.8 eV for Ti to ∼−5.8 eV for Cr. Since the CdO conduction-band minimum (CBM) is located at −5.9 eV, these TM dopant donor levels typically lie above the CdO CBM and can dope CdO by dropping an electron from the d-level to the conduction band. Yang *et al.* compared properties of In-doped CdO with 3d TM dopants (Y and Sc) [31]. They found that while both Y and Sc increase the electron concentration in CdO up to $\sim 7\times10^{20}$ cm^{-3}, the electron mobility dropped to <10 cm^2/Vs with increasing dopant concentration. This is in contrast to In-doped CdO, which showed a high mobility of ∼70 cm^2/Vs for In concentration >8 %. They attributed this to the presence of d-states in Y and Sc, which affect the CB dispersion of CdO.

In this work, we studied the doping of CdO with different transition metal (TM) elements with partially filled 3d or 4d orbitals, namely Sc, Ti, V, Cr, Fe, and Y. The doped CdO thin films were grown by radiofrequency (rf) magnetic sputtering (Ti,V,Y) and pulsed filtered cathodic arc deposition (PFCAD) (Sc, Ti, Cr, Fe). We show that TM dopants act as donor dopants in CdO, and when the dopant concentration is high enough the d-states can modify the electronic band structures of CdO. Such a modification affects both the electrical and optical properties of CdO. The maximum electron concentration achieved through TM doping is related to the position of the localized donor d-levels of different transition metal elements.

II. EXPERIMENT

TM-doped CdO thin films were synthesized by two different methods, namely radiofrequency magnetron sputtering and pulsed filtered cathodic arc deposition (PFCAD) [41]. The Ti-, Fe-, Cr-, and Sc-doped CdO were deposited by dual cathode PFCAD. Films were deposited on soda lime microscope glass slides at 250° C with pure oxygen (O_2) background pressure of about 5 mTorr. The ratio of transition metal elements and Cd can be controlled by the pulsing sequence of the respective metallic cathodes. The pulse duration is 1 ms with a current amplitude of 600 A. The rate of the pulse is 1 pulse per second. A total of 1200–1800 pulses were used for each sample. Ti-, V-, and Y-doped CdO were deposited by rf magnetron sputtering. A TiO_2, V_2O_3, and Y_2O_3 ceramic target were cosputtered with a CdO target for Ti, V, and Y doping, respectively. The composition of the dopants was controlled by varying the power of the dopant targets. The films were also deposited on soda lime microscope glass slides at either room temperature or 270° C with pure argon (Ar) pressure of about 5 mTorr. The deposition time was varied from 15 to 20 min to achieve a film thickness of ∼100 − 200 nm.

The composition and thickness of the samples were measured by Rutherford backscattering spectrometry (RBS) using a 3.04 MeV He^{2+} ion beam at a backscattering angle of 165°. The thickness of the films ranged from 100 to 200 nm. A typical RBS spectrum from a 157 nm CdO doped with ∼3.2% V is shown in Fig. S1 in the supplemental material [42]. The RBS spectra were analyzed using the software package SIMNRA [43]. The crystal structure of the films was determined by x-ray diffraction (XRD). Figure S2 in [42] shows an XRD pattern from the same sample as in Fig. S1. Diffraction peaks from the (111) and (200) planes of rocksalt CdO can be clearly observed. The relatively sharp peaks with high intensity suggest that the samples are polycrystalline with an average grain size of ∼20 nm as estimated from the peak width using Scherrer's equation. Electrical properties were determined by Hall effect measurements in the van der Pauw geometry using an Ecopia HMS3000 system with a 0.55 T magnet at room temperature. Room-temperature optical properties of the films were determined from optical transmission and reflectance spectra measured with a Perkin-Elmer Lambda 950 spectrophotometer.

III. RESULTS AND DISCUSSION

Figure 1(a) shows the electron concentration N, (b) the mobility μ, and (c) the resistivity ρ of CdO doped with increasing concentration of TM elements x from 0 to 10 mol %. The effects of TM dopants, including Sc, Ti, V, Cr, Fe, Y, Mo, and W, are directly compared to In dopants. Note that CdO thin films doped with Mo and W were sputter-deposited at room temperature followed by rapid thermal annealing at 300 °C for 600 s in N_2. In general, similar to In doping, the N increases with increasing TM dopant concentration and reaches a maximum N (N_{max}) of $\sim(7–12)\times10^{20}$ cm^{-3} with a dopant concentration x_{max} of 4–7 %. This confirms that TM elements with partially filled d orbitals (3d or 4d) are effective donors in CdO, and possibly also for other wide-gap oxides such as In_2O_3, SnO_2, and ZnO. However, the μ of CdO films doped with all TM elements drops sharply to as low as <10 cm^2/Vs as x increases. The strong reduction in μ with x was reported previously for Sc-, Y-, and V-doped CdO [31,38,39]. This is in stark contrast to CdO films doped with In (and also Ga) which maintain a high μ of ∼100 cm^2/Vs even with $x \sim$ 10 % [31,34,44]. Hence, the decrease of μ with increasing x in CdO:TM cannot be explained by an increase in ionized impurity scattering. As a direct consequence, the minimum resistivity ρ of CdO:TM films is $\sim(1–2)\times10^{-4}\,\Omega$ cm, which is comparable to most conventional TCOs [1–3]. In contrast, because of the high N_{max} and μ, CdO:In can achieve a ρ as low as $5\times10^{-5}\,\Omega$ cm.

The lower μ for CdO:TM would also affect their optical properties. As an example, Fig. 2 compares optical properties of CdO:In and CdO:Ti films with different x. Figures 2(a)–2(c) show, respectively, the transmittance, reflectance, and absorption for CdO:In films with different x. The ρ and N for the different films are given in parentheses in the legend of Figs. 2(a) and 2(b), respectively. Similar plots for CdO:Ti are

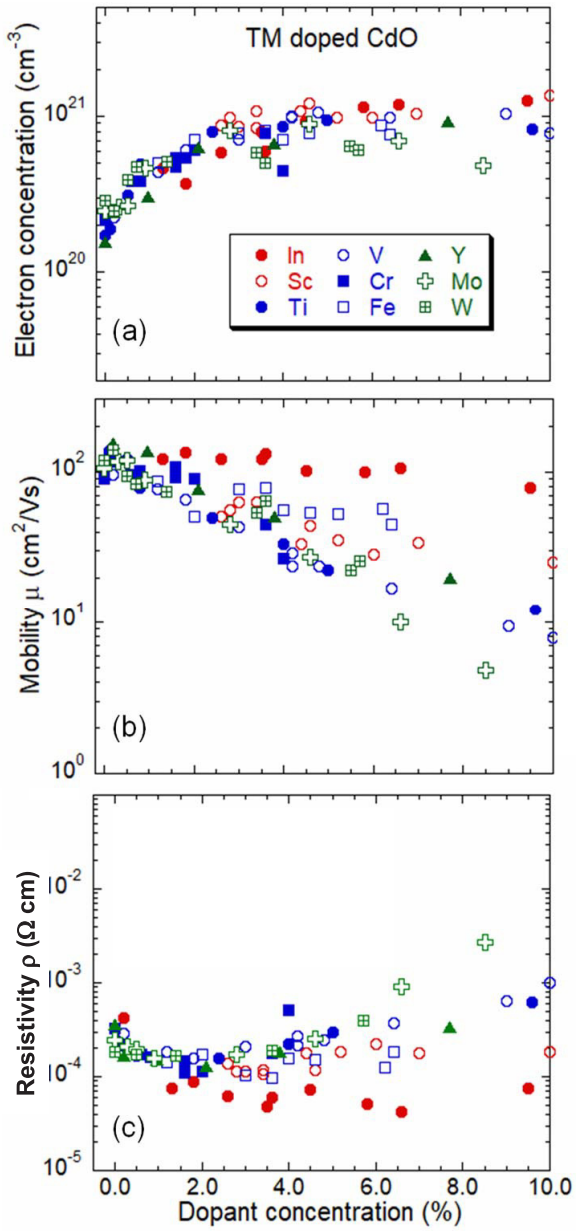

FIG. 1. A comparison of electrical properties: (a) electron concentration N, (b) mobility μ, and (c) resistivity ρ of CdO thin films doped with In and various TM dopants (Sc, Ti, V, Cr, Fe, Y, Mo, and W).

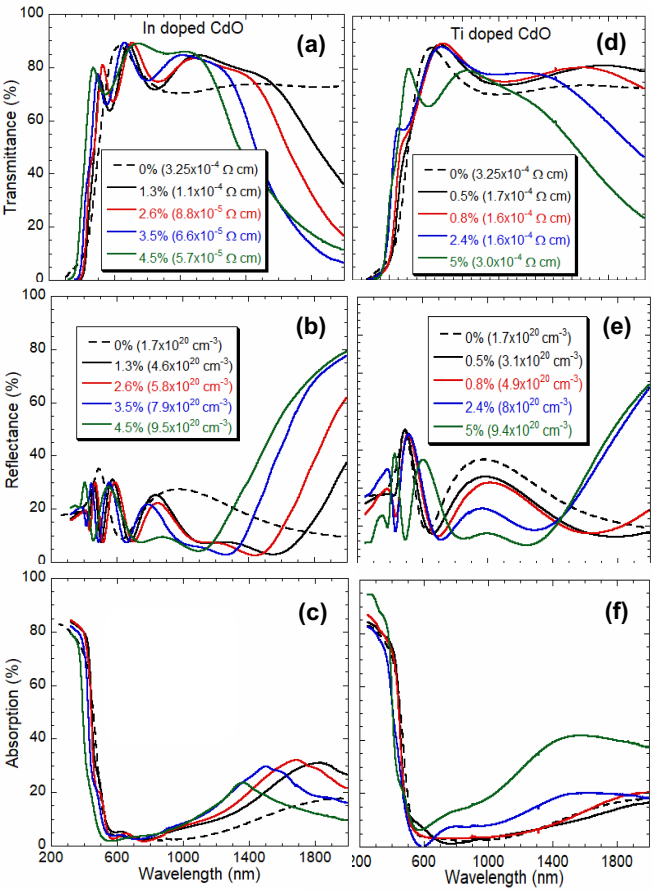

FIG. 2. A comparison of optical properties of In-doped [(a) transmittance, (b) reflectance, and (c) absorption] and Ti-doped [(d) transmittance, (e) reflectance, and (f) absorption] CdO thin films. The resistivity ρ and electron concentration N of the films is given in parentheses in the figure legend of (a), (d) and (b), (e), respectively.

shown in Figs. 2(d)–2(f). Figure 2(a) shows that the CdO:In film with $x = 4.5$ % has a very low $\rho \sim 5.7 \times 10^{-5}\,\Omega\,\text{cm}$ and a high transmittance T up to $\lambda \sim 1200$ nm. The drop in T at $\lambda > 1200$ nm is related to the high $N \sim 9.5 \times 10^{20}\,\text{cm}^{-3}$ in the sample, which gives rise to a strong free-carrier absorption (FCA) [Fig. 2(c)] and plasma reflection [Fig. 2(b)] at high λ. As a comparison, the CdO:Ti film with $x = 5$ % has a comparable $N \sim 9.4 \times 10^{20}\,\text{cm}^{-3}$ but its T drops at a much shorter λ of 1000 nm. This is attributed to the much stronger FCA due to its low $\mu \sim 22\,\text{cm}^2/\text{Vs}$. Using the classical Drude model, the FCA coefficient α_{FCA} can be expressed as

$$\alpha_{\text{FCA}} = \frac{e^3\lambda^2 N}{4\pi^2\mu m_e^{*2} n\varepsilon_0 c^3}, \tag{1}$$

where e is the electron charge, N is the carrier concentration, ε_0 is the static dielectric constant, n is the refractive index, m_e^* is the electron effective mass, and c is the speed of light. Comparing the absorption at $\lambda = 1200$ nm, the In- and Ti-doped CdO with $N \sim 9.4 \times 10^{20}\,\text{cm}^{-3}$ is 15% and 30%, respectively. Figure 3 compares the transmittance spectra of several TM-doped CdO with $x \sim 3 - 4$ % and a similar $\rho \sim 2 \times 10^{-4}\,\Omega\,\text{cm}$ with a CdO:In film with a much lower $\rho \sim 8 \times 10^{-5}\,\Omega\,\text{cm}$. While CdO:TM films are transparent up to $\lambda \sim 1200$ nm, the CdO:In film with a factor of ~3 lower ρ has a transparency window extending to $\lambda > 1400$ nm. Hence, although TM elements are effective donors in CdO, because of their lower μ, their optical properties are not as desirable.

When the electron concentration is high ($N > 10^{19}\,\text{cm}^{-3}$) in a semiconductor, carrier filling of the conduction band results in a blueshift [or Burstein-Moss shift (ΔE_{BM})] in the absorption edge. At the same time, electron-electron interaction (ΔE_{e-e}) and ion-electron interaction (ΔE_{i-e}) [45,46] give rise to a redshift (band renormalization, ΔE_{BR}) that is significantly smaller in magnitude than the ΔE_{BM}. Therefore, the measured optical absorption edge (E_{opt}) is related to the intrinsic band gap E_G

$$E_{\text{opt}} = E_G + \Delta E_{\text{BM}} - (\Delta E_{e-e} + \Delta E_{i-e}). \tag{2}$$

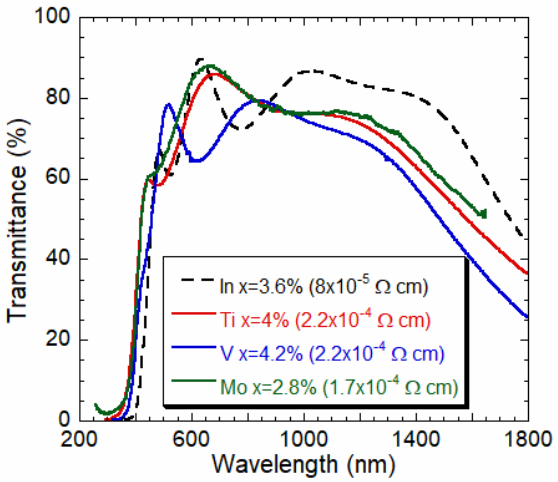

FIG. 3. Transmittance of In-doped and TM-doped CdO thin films with dopant concentration $x \sim 3-4$ %. The resistivities of the films are given in parentheses in the figure legend.

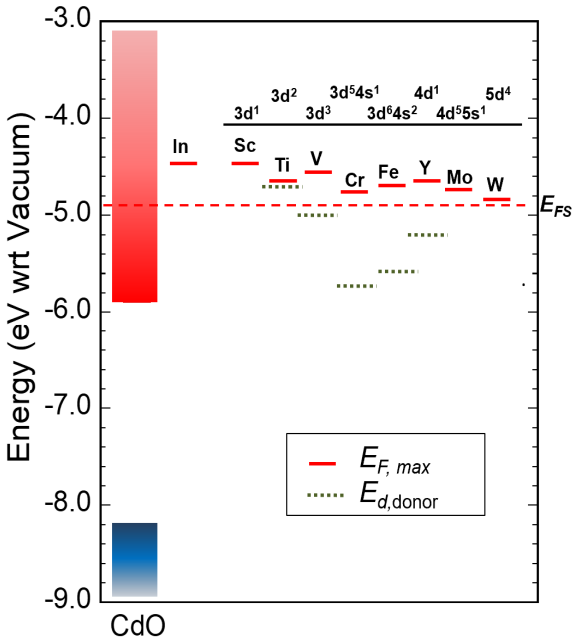

FIG. 4. A schematic diagram showing the Fermi level positions $E_{F,\max}$ (red lines) for In- and TM-doped CdO with $N_{\max}$. Energy positions of the corresponding d donor levels $E_{d,\text{donor}}$ (green dotted lines) and the Fermi level stabilization energy E_{FS} (red dashed line) are also shown.

The ΔE_{BM} which is the energy separation between the CBM and the Fermi level E_F or (E_F–E_C) can be calculated using the nonparabolic conduction-band model [47,48], while the band renormalization is evaluated by Jain's model [49]. Table I compares the electrical properties of the In and Ga doped with TM-doped CdO films at their respective maximum N ($N_{\max}$). The position of the E_{F} ($E_{F,\max}$) with respect to E_C as well as E_{vac} are also tabulated. Notice that compared to Ga- and In-doped CdO, TM-doped films with $x_{\max}$ have significantly higher ρ due to their low μ.

Figure 4 is a schematic diagram showing the Fermi level positions $E_{F,\max}$ (red lines) for In- and TM-doped CdO with $N_{\max}$. Energy positions of the corresponding d donor levels $E_{d,\text{donor}}$ (green dotted lines) and the Fermi level stabilization energy E_{FS} (red dashed line) are also shown. The Fermi level stabilization energy is the Fermi level at which the formation energies of donor- and acceptor-type native defects in a semiconductor are equal, and it is located at ~4.9 eV below E_{vac} [50–53]. Consequently, when a semiconductor is doped n- (p-) type with the E_{F} above (below) E_{FS}, the formation of compensating native acceptors (donors) becomes favorable, hence limiting the maximum doping of a semiconductor. Typically, a semiconductor can be doped n–(p–) type with E_{F} within ~1 eV above (below) E_{FS} [54,55]. Langer *et al.* [40] showed that d shell derived states are localized states that remain relatively constant with respect to E_{vac} and compiled energy levels of several d-donor ($E_{d,\text{donor}}$) and d-acceptor ($E_{d,\text{acceptor}}$) states in II-VI compounds. The $E_{d,\text{donor}}$ levels for several TM elements are also shown in Fig. 4 as green dotted lines. Note that $E_{F,\max}$ of all the TM dopants lie higher than E_{FS} so that a significant amount of compensating native acceptors are present in the films with $N_{\max}$. This may contribute to the lower μ found in these films. Moreover, for most 3d TM dopants, higher $E_{d,\text{donor}}$ gives rise to higher $E_{F,\max}$. Figure 5

TABLE I. A summary of the mobility μ, resistivity ρ, dopant concentration $x_{\max}$, the $E_{F,\max}$ and ΔE_{BR} for CdO films doped with TM, as well as In and Ga with maximum N ($N_{\max}$). The last column lists the position of the $E_{F,\max}$ with respect to the vacuum level (E_{vac}) by assuming that the E_{vac}–E_C (or the electron affinity) of CdO is 5.9 eV.

Dopant	$N_{\max}$ ($\times 10^{20}$ cm^{-3})	μ (cm^2/V s)	ρ ($\times 10^{-4}$ Ω cm)	$x_{\max}$ (%)	$E_{F,\max}$–E_c (eV)	ΔE_{BR} (eV)	$E_{F,\max} - E_{\text{vac}}$ (eV)
Ga	9.3	90	0.748	4.4	1.26	0.405	–4.64
In	11.9	106	0.495	6.6	1.41	0.43	–4.49
Sc	12	44	1.18	4.6	1.41	0.43	–4.49
Ti	9.4	22.4	2.97	4	1.27	0.41	–4.63
V	10.8	23.8	2.43	4.8	1.34	0.42	–4.56
Fe	8.78	56.8	1.25	6.2	1.21	0.4	–4.69
Cr	7.76	44.9	1.79	3.6	1.13	0.4	–4.77
Y	9.3	20	3.36	7.7	1.25	0.405	–4.65
Mo	8.98	27.6	2.52	4.6	1.24	0.4	–4.66
W	6.43	22.5	4.32	5.5	1.05	0.38	–4.85

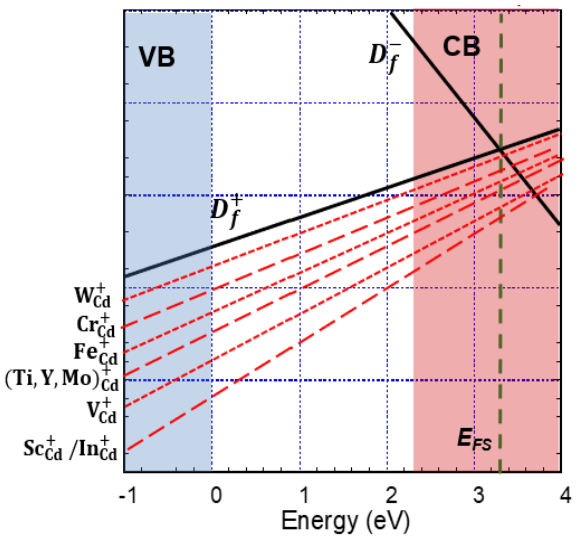

FIG. 5. A schematic energy diagram showing the formation energies of various substitutional dopants in CdO as estimated from their $E_{F,\max}$.

shows a schematic energy diagram showing the formation energies of various substitutional dopants in CdO as estimated from their $E_{F,\max}$, where D_f^- and D_f^+ are the singly charged native acceptor and donor, respectively. In CdO, D_f^- and D_f^+ are most likely Cd vacancy (V_{Cd}) and O interstitial O_i [30]. Note that the formation energies of the substitutional dopants are significantly lower than that of the native donors even at E_{FS}.

The optical gap E_{opt} of the CdO films was obtained by extrapolating the α^2 versus photon energy plots to the energy intercept. Figure 6 shows the N and E_{opt} of CdO:TM (Ti,V,Mo) compared to CdO:In as a function of x. For CdO:In, both N and E_{opt} increase with x, consistent with the BM effect. However, for films doped with TM elements, at high x, the

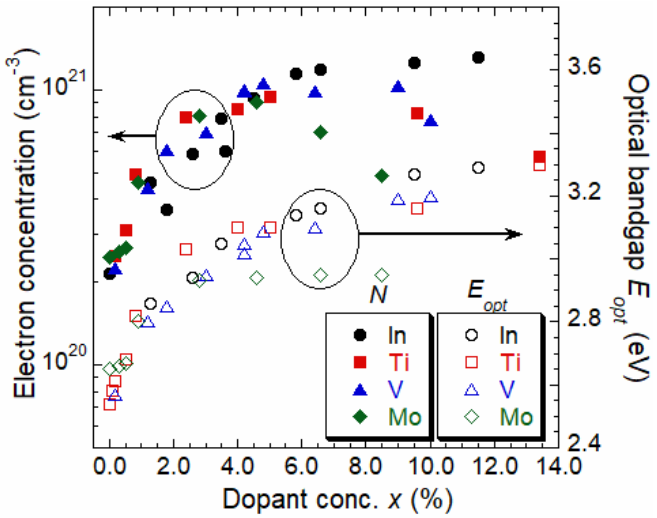

FIG. 6. The electron concentration N and optical gap E_{opt} of TM (Ti,V,Mo) compared to In-doped CdO as a function of dopant concentration x.

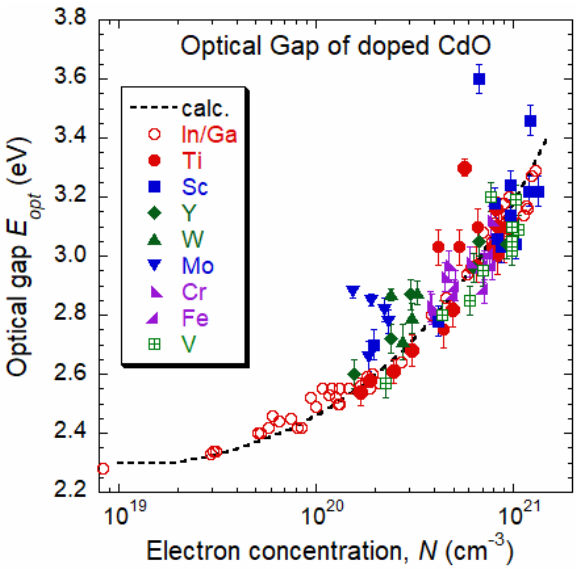

FIG. 7. The E_{opt} of CdO thin films undoped and doped with TM elements as compared to those doped with In and Ga. The calculated E_{opt} taking into account BM shift and band renormalization effects is shown as the dashed curve.

N decreases while E_{opt} either saturates (Mo) or continues to increase (Ti and V). This suggests that the TM dopants modify the electronic band structure so that the E_{opt} in these samples is no longer entirely determined by free carriers at high x. Garcia-Hemme *et al.* studied V doping in ZnO and showed that localized V d-levels modify the CB of ZnO [56] through the anticrossing interaction between the V d-levels and CB extended states of the ZnO. Such interaction results in the splitting of the CB into a mostly unoccupied upper CB (E_+ subband) and a lower broadened occupied narrow band (E_- subband). This band anticrossing (BAC) model was developed to describe the modification of the CB and VB of highly mismatched alloys (HMAs) (e.g., dilute GaN_xAs_{1-x}) in which metallic anions (e.g., As in GaAs) in a compound semiconductor are partially replaced with more electronegative atoms (e.g., N) [57–59]. The increasing E_{opt} with x for TM dopants shown in Fig. 6 even at high x when N drops cannot be explained by the BM effect, but it is consistent with the BAC model where localized d-states of TM dopants interact with extended CB states of CdO. E_{opt} in these CdO:TM films at high x correspond to transitions from the VB to the unoccupied E_+.

Figure 7 shows E_{opt} with increasing N for CdO thin films undoped and doped with In, Ga, and the various TM elements. The dashed line shows the calculated E_{opt} with free-carrier effects (namely BM shift and band renormalization) [47,49,53,60] taken into account by assuming an intrinsic gap of 2.3 eV for CdO. Note that for the Ga- and In-doped CdO, the experimental E_{opt} follows the calculated values closely, which confirms that the increased E_{opt} in these samples with N can be fully explained by free-carrier effects. However, for CdO:TM, although E_{opt} follows the calculated values at low x, as x increases the CB of CdO is modified by the anticrossing interaction, and hence E_{opt} values are significantly higher than the calculated values.

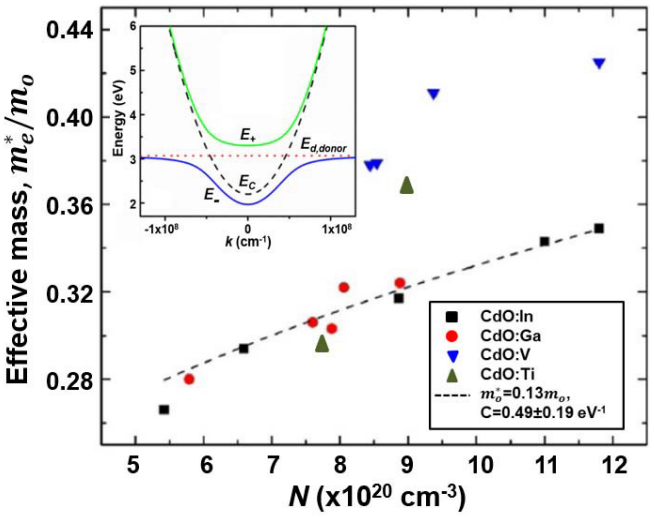

FIG. 8. Electron effective mass m_e^* for CdO derived from spectroscopic ellipsometry measurements for CdO with different dopants. The black dashed line is the best fit for the In- and Ga-doped samples according to Eq. (3). The inset shows the dispersion of the restructured conduction band due to band anticrossing between the TM d-states ($E_{d,\mathrm{donor}}$) and CdO CB (E_C).

Because of the anticrossing interactions of the localized d-states and the extended CB states, the dispersion of both the E_+ and E_- subbands is significantly flattened. The dispersion shown in the inset of Fig. 8 illustrates the band restructuring due to the anticrossing interaction. Since the electron effective mass m_e^* is related to the reciprocal of the derivative of the CB dispersion, m_e^* for the CdO:TM films is also significantly larger because of the flatter band dispersion. Figure 8 shows the effective mass for the CdO films doped with In, Ga, V, and Ti as a function of N extracted from spectroscopic ellipsometry (SE) measurements [35]. For the CdO films doped with In and Ga, the dependence of the m_e^* on the electron concentration N follows the nonparabolic conduction-band model [47,48],

$$m_e^* = m_o^* \sqrt{1 + 2C\frac{\hbar^2}{m_o^*}(3\pi^2 N)^{\frac{2}{3}}}. \tag{3}$$

where m_o^* is the effective mass at the bottom of the conduction band and C is a nonparabolicity parameter. A best fit of the data from CdO samples doped with In and Ga (dashed line in Fig. 8) using Eq. (3) shows $m_o^* = 0.13m_o$ and $C = 0.49\,\mathrm{eV}^{-1}$, with m_o being the free-electron mass. However, at high N, values of m_e^* for V- and Ti-doped CdO deviate significantly from the fit and cannot be described by Eq. (3). The much higher m_e^* for the Ti- and V-doped films are consistent with the much flatter restructured CdO CB as shown in the inset of Fig. 8, and it can explain the much lower μ of these samples at high N shown in Fig. 1.

In contrast to previous reports on the mobility enhancement of In_2O_3 doped with transition metal species, such a desirable effect in CdO:TM studied in this work is rather subtle, if not totally absent. Note that mobility is related to the mean free time of carrier scattering τ and electron effective mass m_e^* ($\mu = e\tau/m_e^*$). Since the m_e^* of CdO is only slightly smaller than that of In_2O_3, the inherently high μ of CdO originates primarily from the reduced scattering (increase in τ) due to its high static dielectric constant ($\varepsilon_o \sim 22$ for CdO as compared to 8.9 for In_2O_3) which effectively screens ionized impurity centers. Swallow *et al.* [20] suggested that the much higher μ of Mo-doped In_2O_3 compared to ITO arises from its smaller m_e^* due to resonant Mo 4d states, which do not perturb the host CBM. In CdO, this effect, if present, becomes relatively insignificant when compared to the effect due to carrier scattering since the electron scattering cross section $\sigma \propto 1/\varepsilon_o^2$. Nevertheless, in several cases, e.g., Ti, Mo, and W doping of CdO, a slight increase in the μ is still visible when the dopant concentration is <1 %. Only when the dopant concentration is >2 % does the mobility drop significantly, which we attribute to the flattening of the CB due to the anticrossing interaction of dopant d states and CB extended states. In fact, despite the increase in μ for In_2O_3 with moderate TM dopant concentration, it was also reported that a reduction in μ is observed at high dopant concentration [18,22,24,61,62]. The difference in the exact dopant concentration where the reduction of μ occurs may depend on the TM dopant species and/or film deposition methods and conditions. For CdO, TM donors such as Sc, Y, Lu, and La with nd^1 outer electron after using the 2 $(n–1)s^2$ electrons for bonding would be good potential donors. However, the exact orbital energy levels of these dopants are not accurately known, and therefore theoretical calculations are required to fully understand these experimental results and give a more complete picture on the TM doping in CdO.

IV. CONCLUSION

In this work, we explore a series of transition metal (TM) elements with partially filled 3d and 4d shells, including Sc, Ti, V, Cr, Fe, Y, Mo, and W, as possible donors in CdO (CdO:TM). We find that these TM elements can act as effective donors in CdO with the electron concentration N increasing to a maximum N ($N_{\max}$) of $\sim(7-12)\times10^{20}\,\mathrm{cm}^{-3}$ with a dopant concentration $x_{\max}$ of 4–7 %, comparable to CdO doped with In. Because of the high $N_{\max}$, the corresponding Fermi levels $E_{F,\max}$ lie higher than the CdO conduction-band minimum (CBM) (>1 eV). In general, we also find that TM dopant with a higher d-donor level $E_{d,\mathrm{donor}}$ gives rise to a higher $N_{\max}$, and thus also a higher $E_{F,\max}$. However, in contrast to CdO:In, which has a high mobility μ of $>100\,\mathrm{cm}^2/\mathrm{Vs}$ even with $N>10^{21}\,\mathrm{cm}^{-3}$, the μ in CdO:TM films drops rapidly to $<20\,\mathrm{cm}^2/\mathrm{Vs}$ as the dopant concentration x increases to >4 %. As a result, CdO:TM films have a minimum ρ of $(1–2)\times10^{-4}\,\Omega\,\mathrm{cm}$, a factor of $\sim2-3$ higher than that of CdO:In. The low μ of CdO:TM increases the free-carrier absorption at high N, and hence limits the optical transparency to <1200 nm. Finally, unlike undoped and In-doped CdO where the optical band gap E_{opt} is determined by free-carrier effects, namely BM shift and band renormalization, in TM-doped CdO, as x increases, E_{opt} values are significantly higher than the calculated values. This is believed to be the effect of the anticrossing interaction of the localized d-levels and the extended CdO CB states, giving rise to lower occupied E_- and upper unoccupied E_+ subbands. The observed E_{opt} in CdO:TM arises from electrons

transitioning from the VB to the unoccupied E_+ subband. The restructured CBs have much flatter dispersion, which results in a much higher effective mass m_e^*, and this also explains the much lower μ observed in CdO:TM films with high N.

ACKNOWLEDGMENTS

The work performed at LBNL was supported by the Director, Office of Science, Office of Basic Energy Sciences, Materials Sciences and Engineering Division, of the U.S. Department of Energy under Contract No. DE-AC02-05CH11231. K.M.Y. was supported by CityU SGP project No. 9380076. Y.J.L. was supported by the China Scholarship Council, National Natural Science Foundation of China (No. 51602121), and the Ph.D. Start-up Program of Huizhou University (No. 2016JB006). G.C. acknowledges support from National Natural Science Foundation of China (No. 11174101), and C.P.L. acknowledges the support from Department of Science and Technology of Guangdong Province under Project No. 2021A0505030081.

[1] *Handbook of Transparent Conductors*, edited by D. S. Ginley, H. Hosono, and D. C. Paine (Springer, New York, 2011).

[2] J. Robertson, R. Gillen, and S. J. Clark, Advances in understanding of transparent conducting oxides, Thin Solid Films **520**, 3714 (2012).

[3] K. Ellmer, Past achievements and future challenges in the development of optically transparent electrodes, Nat. Photon. **6**, 809 (2012).

[4] S. C. Dixon, D. O. Scanlon, C. J. Carmalt, and I. P. Parkin, n-Type doped transparent conducting binary oxides: An overview, J. Mater. Chem. C **4**, 6946 (2016).

[5] M. Morales-Masis, S. De Wolf, R. Woods-Robinson, J. W. Ager, and C. Ballif, Transparent electrodes for efficient optoelectronics, Adv. Electron. Mater. **3**, 1600529 (2017).

[6] Z. Wang, C. Chen, K. Wu, H. Chong, and H. Ye, Transparent conductive oxides and their applications in near infrared plasmonics, Phys. Status Solidi A **216**, 1700794 (2019).

[7] H. Kim, C. M. Gilmore, A. Pique, J. S. Horwitz, H. Mattoussi, H. Murata, Z. H. Kafafi, and D. B. Chrisey, Electrical, optical, and structural properties of indium–tin–oxide thin films for organic light-emitting devices, J. Appl. Phys. **86**, 6451 (1999).

[8] K. L. Chopra, P. D. Paulson, and V. Dutta, Thin-film solar cells: An overview, Prog. Photovolt: Res. Appl. **12**, 69 (2004).

[9] N. Romeo, A. Bosio, V. Canevari, M. Terheggen, and L. V. Roca, Comparison of different conducting oxides as substrates for CdS/CdTe thin film solar cells, Thin Solid Films **431**, 364 (2003).

[10] J. T. Lim, C. H. Jeong, A. Vozny, J. H. Lee, M. S. Kim, and G. Y. Yeom, Top-emitting organic light-emitting diode using transparent conducting indium oxide layer fabricated by a two-step ion beam-assisted deposition, Surf. Coat. Technol. **201**, 5358 (2007).

[11] J. Müller, B. Rech, J. Springer, and M. Vanecek, TCO and light trapping in silicon thin film solar cells, Sol. Energy **77**, 917 (2004).

[12] S. Faÿ, J. Steinhauser, N. Oliveira, E. V. Sauvain, and C. Ballif, Opto-electronic properties of rough LP-CVD ZnO:B for use as TCO in thin-film silicon solar cells, Thin Solid Films **515**, 8558 (2007).

[13] A. E. Delahoy and S. Y. Guo, Transparent conducting oxides for photovoltaics, in *Handbook of Photovoltaic Science and Engineering*, edited by A. Luque and S. Hegedus (Wiley, Chichester, 2011), pp. 716–796.

[14] R. G. Gordon, Technological challenges for transparent conductors, Adv. Sci. Technol. (Faenza, Italy) **33**, 1037 (2003).

[15] J.-i. Nomoto, T. Hirano, T. Miyata, and T. Minami, Preparation of Al-doped ZnO transparent electrodes suitable for thin-film solar cell applications by various types of magnetron sputtering depositions, Thin Solid Films **520**, 1400 (2011).

[16] O. Bierwagen, Indium oxide—A transparent, wide-band gap semiconductor for (Opto)electronic applications, Semicond. Sci. Technol. **30**, 024001 (2015).

[17] J. E. N. Swallow, B. A. D. Williamson, T. J. Whittles, M. Birkett, T. J. Featherstone, N. Peng, A. Abbott, M. Farnworth, K. J. Cheetham, P. Warren, D. O. Scanlon, V. R. Dhanak, and T. D. Veal, Self-compensation in transparent conducting F-doped SnO_2, Adv. Funct. Mater. **28**, 1701900 (2017).

[18] M. F. A. M. van Hest, M. S. Dabney, J. D. Perkins, and D. S. Ginley, High-mobility molybdenum doped indium oxide, Thin Solid Films **496**, 70 (2006).

[19] R. Hashimoto, Y. Abe, and T. Nakada, High mobility titanium-doped In_2O_3 thin films prepared by sputtering/post-annealing technique, Appl. Phys. Exp. **1**, 015002 (2008).

[20] J. E. N. Swallow, B. A. D. Williamson, S. Sathasivam, M. Birkett, T. J. Featherstone, P. A. E. Murgatroyd, H. J. Edwards, Z. W. Lebens-Higgins, D. A. Duncan, M. Farnworth, N. Peng, P. Warren, T. L. Lee, L. F. J. Piper, A. Regoutz, C. J. Carmalt, I. P. Parkin, V. R. Dhanak, D. O. Scanlon, and T. D. Veal, Resonant doping for high mobility transparent conductors: The case of Mo-doped In_2O_3, Mater. Horiz. **7**, 236 (2020).

[21] P. F. Newhouse, C. H. Park, D. A. Keszler, J. Tate, and P. S. Nyholm, High electron mobility W-doped In_2O_3 thin films by pulsed laser deposition, Appl. Phys. Lett. **87**, 112108 (2005).

[22] T. Koida and M. Kondo, High-mobility transparent conductive Zr-doped In_2O_3, Appl. Phys. Lett. **89**, 082104 (2006).

[23] F. Meng, J. Shi, Z. Liu, Y. Cui, Z. Lu, and Z. Feng, High mobility transparent conductive W-doped In_2O_3 thin films prepared at low substrate temperature and its application to solar cells, Sol. Energy Mater. Sol. Cells **122**, 70 (2014).

[24] K. O. Egbo, A. E. Adesina, C. V. Ezeh, C. P. Liu, and K. M. Yu, Effects of free carriers on the optical properties of high mobility transition metal doped In_2O_3 transparent conductors, Phys. Rev. Mater. **5**, 094603 (2021).

[25] T. Koida, M. Kondo, K. Tsutsumi, A. Sakaguchi, M. Suzuki, and H. Fujiwara, Hydrogen-doped In_2O_3 transparent conducting oxide films prepared by solid-phase crystallization method, J. Appl. Phys. **107**, 033514 (2010).

[26] B. Macco, H. C. M. Knoops, and W. M. M. Kessels, Electron scattering and doping mechanisms in solid-phase-crystallized

In_2O_3:H prepared by atomic layer deposition, ACS Appl. Mater. Interf. **7**, 16723 (2015).

[27] S. Husein, M. Stuckelberger, B. West, L. Ding, F. Dauzou, M. Morales-Masis, M. Duchamp, Z. Holman, and M. I. Bertoni, Carrier scattering mechanisms limiting mobility in hydrogen-doped indium oxide, J. Appl. Phys. **123**, 245102 (2018).

[28] B. A. D. Williamson, T. J. Featherstone, S. S. Sathasivam, J. E. N. Swallow, H. Shiel, L. A. H. Jones, M. J. Smiles, A. Regoutz, T.-L. Lee, X. Xia, C. Blackman, P. K. Thakur, C. J. Carmalt, I. P. Parkin, T. D. Veal, and D. O. Scanlon, Resonant Ta doping for enhanced mobility in transparent conducting SnO_2, Chem. Mater. **32**, 1964 (2020).

[29] M. Yan, M. Lane, C. R. Kannewurf, and R. P. H. Chang, Highly conductive epitaxial CdO thin films prepared by pulsed laser deposition, Appl. Phys. Lett. **78**, 2342 (2001).

[30] M. Burbano, D. O. Scanlon, and G. W. Watson, Sources of conductivity and doping limits in CdO from hybrid density functional theory, J. Am. Chem. Soc. **133**, 15065 (2011).

[31] Y. Yang, S. Jin, J. E. Medvedeva, J. R. Ireland, A. W. Metz, J. Ni, M. C. Hersam, A. J. Freeman, and T. J. Marks, CdO as the archetypical transparent conducting oxide: Systematics of dopant ionic radius and electronic structure effects on charge transport and band structure, J. Am. Chem. Soc. **127**, 8796 (2005).

[32] E. Sachet, C. T. Shelton, J. S. Harris, B. E. Gaddy, D. L. Irving, S. Curtarolo, J. Ihlefeld, S. Franzen, J.-P. Maria, B. F. Donovan, P. E. Hopkins, P. A. Sharma, and A. L. Sharma, Dysprosium-doped cadmium oxide as a gateway material for mid-infrared plasmonics, Nat. Mater. **14**, 414 (2015).

[33] S. Jin, Y. Yang, J. E. Medvedeva, L. Wang, S. Li, N. Cortes, J. R. Ireland, A. W. Metz, J. Ni, M. C. Hersam, A. J. Freeman, and T. J. Marks, Tuning the properties of transparent oxide conductors. dopant ion size and electronic structure effects on CdO-Based Transparent Conducting Oxides. Ga- and In-Doped CdO thin films grown by MOCVD, Chem. Mater. **20**, 220 (2008).

[34] K. M. Yu, M. A. Mayer, D. T. Speaks, H. He, R. Zhao, L. Hsu, S. S. Mao, E. E. Haller, and W. Walukiewicz, Ideal transparent conductors for full spectrum photovoltaics, J. Appl. Phys. **111**, 123505 (2012).

[35] C. P. Liu, Y. Foo, M. Kamruzzaman, C. Y. Ho, J. A. Zapien, W. Zhu, Y. J. Li, W. Walukiewicz, and K. M. Yu, Effects of Free Carriers on the Optical Properties of Doped Cdo for Full-Spectrum Photovoltaics, Phys. Rev. Appl. **6**, 064018 (2016).

[36] R. K. Gupta, K. Ghosh, R. Patel, and P. K. Kahol, Highly conducting and transparent Ti-doped CdO films by pulsed laser deposition, Appl. Surf. Sci. **255**, 6252 (2009).

[37] K. P. Kelley, E. Sachet, C. T. Shelton, and J. -P. Maria, High mobility yttrium doped cadmium oxide thin films, APL Mater. **5**, 076105 (2017).

[38] Y. J. Li, K. M. Yu, G. B. Chen, C. P. Liu, and W. Walukiewicz, Conduction band modifications by d states in vanadium doped CdO, J. Alloy. Compd. **822**, 153567 (2020).

[39] M. Xie, W. Zhu, K. M. Yu, Z. Zhu, and G. Wang, Effects of doping and rapid thermal processing in Y doped CdO thin films, J. Alloy. Compd. **776**, 259 (2019).

[40] J. M. Langer, C. Delerue, M. Lannoo, and H. Heinrich, Transition-metal impurities in semiconductors and heterojunction band lineups, Phys. Rev. B **38**, 7723 (1988).

[41] A. Anders, Energetic deposition using filtered cathodic arc plasmas, Vacuum **67**, 673 (2002).

[42] See Supplemental Material at http://link.aps.org/supplemental/10.1103/PhysRevMaterials.7.074602 for a Rutherford backscattering spectrum and an x-ray diffraction pattern of a representative CdO:V thin film.

[43] M. Mayer, *SIMNRA User's Guide*, Report IPP 9/113 (Max-Planck-Institut für Plasmaphysik, Garching, Germany, 1997).

[44] K. M. Yu, D. M. Detert, G. Chen, W. Zhu, C. P. Liu, S. Grankowska, L. Hsu, O. D. Dubon, and W. Walukiewicz, Defects and properties of cadmium oxide based transparent conductors, J. Appl. Phys. **119**, 181501 (2016).

[45] J. Wu, W. Walukiewicz, W. Shan, K. M. Yu, J. W. Ager III, E. E. Haller, H. Lu, and W. J. Schaff, Effects of the narrow band gap on the properties of InN, Phys. Rev. B **66**, 201403(R) (2002).

[46] K.-F. Berggren and B. E. Sernelius, Band-gap narrowing in heavily doped many-valley semiconductors, Phys. Rev. B **24**, 1971 (1981).

[47] T. Pisarkiewicz, K. Zakrzewska, and E. Leja, Scattering of charge carriers in transparent and conducting thin oxide films with a non-parabolic conduction band, Thin Solid Films **174**, 217 (1989).

[48] T. Pisarkiewicz and A. Kolodziej, Nonparabolicity of the conduction band structure in degenerate tin dioxide, Phys. Status Solidi B **K5**, 158 (1990).

[49] S. C. Jain and D. J. Roulston, A simple expression for band gap narrowing (BGN) in heavily doped Si, Ge, GaAs and Ge_xSi_{1-x} strained layers, Solid-State Electron. **34**, 453 (1991).

[50] W. Walukiewicz, Amphoteric native defects in semiconductors, Appl. Phys. Lett. **54**, 2094 (1989).

[51] S. X. Li, K. M. Yu, J. Wu, R. E. Jones, W. Walukiewicz, J. W. Ager III, W. Shan, E. E. Haller, H. Lu, and W. J. Schaff, Fermi-level stabilization energy in group III nitrides, Phys. Rev B **71**, 161201(R) (2005).

[52] D. T. Speaks, M. A. Mayer, K. M. Yu, S. S. Mao, E. E. Haller, and W. Walukiewicz, Fermi level stabilization energy in cadmium oxide, J. Appl. Phys. **107**, 113706 (2010).

[53] D. M. Detert, K. B. Tom, C. Battaglia, J. D. Denlinger, S. H. N. Lim, A. Javey, A. Anders, O. D. Dubon, K. M. Yu, and W. Walukiewicz, Fermi level stabilization and band edge energies in $Cd_xZn_{1-x}O$ alloys, J. Appl. Phys. **115**, 233708 (2014).

[54] W. Walukiewicz, Intrinsic limitations to the doping of wide-gap semiconductors, Physica B **123**, 302 (2001).

[55] J. Robertson and S. J. Clark, Limits to doping in oxides, Phys. Rev. B **83**, 075205 (2011).

[56] E. García-Hemme, K. M. Yu, P. Wahnon, G. González-Díaz, and W. Walukievicz, Effects of the d-donor level of vanadium on the properties of $Zn_{1-x}V_xO$ films, Appl. Phys. Lett. **106**, 182101 (2015).

[57] W. Shan, W. Walukiewicz, J. W. Ager III, E. E. Haller, J. F. Geisz, D. J. Friedman, J. M. Olson, and S. R. Kurtz, Band Anticrossing in GaInNAs Alloys, Phys. Rev. Lett. **82**, 1221 (1999).

[58] W. Walukiewicz, W. Shan, K. M. Yu, J. W. Ager III, E. E. Haller, I. Miotkowski, M. J. Seong, H. Alawadhi, and A. K. Ramdas, Interaction of Localized Electronic States with the Conduction Band: Band Anticrossing in Ii-Vi Semiconductor Ternaries, Phys. Rev. Lett. **85**, 1552 (2000).

[59] J. Wu, W. Shan, and W. Walukiewicz, Band anticrossing in highly mismatched III–V semiconductor alloys, Semicond. Sci. Technol. **17**, 860 (2002).

[60] I. Hamberg, C. G. Granqvist, K. -F. Berggren, B. E. Sernelius, and L. Engström, Band-gap widening in heavily Sn-doped In_2O_3, Phys. Rev. B **30**, 3240 (1984).

[61] S. Parthiban, E. Elangovan, K. Ramamurthi, R. Martins, and E. Fortunato, High near-infrared transparency and carrier mobility of Mo doped In_2O_3 thin films for optoelectronics applications, J. Appl. Phys. **106**, 063716 (2009).

[62] N. Yamada, M. Yamada, H. Toyama, R. Ino, X. Cao, Y. Yamaguchi, and Y. Ninomiya, High-throughput optimization of near-infrared-transparent Mo-doped In_2O_3 thin films with high conductivity by combined use of atmospheric-pressure mist chemical-vapor deposition and sputtering, Thin Solid Films **626**, 46 (2017).